

Blue large-amplitude pulsators as a new class of variable stars

Paweł Pietrukowicz^{1*}, Wojciech A. Dziembowski^{1,2}, Marilyn Latour³, Rodolfo Angeloni^{4,5,6}, Radosław Poleski^{1,7}, Francesco di Mille⁸, Igor Soszyński¹, Andrzej Udalski¹, Michał K. Szymański¹, Łukasz Wyrzykowski¹, Szymon Kozłowski¹, Jan Skowron¹, Dorota Skowron¹, Przemek Mróz¹, Michał Pawlak¹ & Krzysztof Ulaczyk^{1,9}

¹Warsaw University Observatory, Al. Ujazdowskie 4, 00-478 Warszawa, Poland

²Nicolaus Copernicus Astronomical Center, ul. Bartycka 18, 00-716 Warszawa, Poland

³Dr. Karl Remeis-Observatory & ECAP, Astronomical Institute, Friedrich-Alexander University Erlangen-Nuremberg, Sternwartstr. 7, 96049, Bamberg, Germany

⁴Departamento de Física y Astronomía, Universidad de La Serena, Av. Cisternas 1200 Norte, La Serena, Chile

⁵Instituto de Investigación Multidisciplinar en Ciencia y Tecnología, Universidad de La Serena, Av. Raúl Bitrán 1305, La Serena, Chile

⁶Gemini Observatory, Casilla 603, La Serena, Chile

⁷Department of Astronomy, Ohio State University, 140 W. 18th Ave., Columbus, OH 43210, USA

⁸Las Campanas Observatory, Casilla 601, La Serena, Chile

⁹Department of Physics, University of Warwick, Gibbet Hill Road, Coventry, CV4 7AL, UK

*e-mail: pietruk@astrouw.edu.pl

Regular intrinsic brightness variations observed in many stars are caused by pulsations. These pulsations provide information on the global and structural parameters of the star. The pulsation periods range from seconds to years, depending on the compactness of the star and properties of the matter that forms its outer layers. Here, we report the discovery of more than a dozen of previously unknown short-period variable stars: blue large-amplitude pulsators. These objects show very regular brightness variations with periods in the range of 20–40 min and amplitudes of 0.2–0.4 mag in the optical passbands. The phased light curves have a characteristic sawtooth shape, similar to the shape of classical Cepheids and RR Lyrae-type stars pulsating in the fundamental mode. The objects are significantly bluer than main sequence stars observed in the same fields, which indicates that all of them are hot stars. Follow-up spectroscopy confirms a high surface temperature of about 30,000 K. Temperature and colour changes over the cycle prove the pulsational nature of the variables. However, large-amplitude pulsations at such short periods are not observed in any known type of stars, including hot objects. Long-term photometric observations show that the variable stars are very stable over time. Derived rates of period change are of the order of 10^{-7} per year and, in most cases, they

are positive. According to pulsation theory, such large-amplitude oscillations may occur in evolved low-mass stars that have inflated helium-enriched envelopes. The evolutionary path that could lead to such stellar configurations remains unknown.

Thousands of pulsating stars have been discovered in the Milky Way and other galaxies of the Local Group over the last decades, mainly thanks to large-scale variability surveys. The OGLE survey [1] has created the largest ever collection of variable stars [2–6]. In 2016, this collection reached almost a million objects, nearly half of which are pulsating stars. Among the detected pulsators are long-period variables, δ Cephei, RR Lyrae and δ Scuti-type stars. By monitoring about a billion stars in the sky, we are able to find extremely rare objects, such as the blue large-amplitude pulsators (BLAPs) presented here.

The first unusual ultra-short-period variable with a sawtooth light curve was found in the OGLE Galactic Disk field towards the constellation of Carina during our search [7] for variable objects with periods shorter than 1 h, conducted in 2013. Owing to the location in an obscured area of the disk at unknown distance, it was not possible to obtain information on the luminosity of this object. With a period of about 28.26 min and a light curve resembling fundamental-mode pulsators, the star was tentatively classified as a δ Sct-type variable and named OGLE-GD-DSCT-0058. However, its amplitude of about 0.24 mag in the I band was higher than had ever been observed among the shortest-period δ Sct variables. It is several times higher than in a dozen known δ Sct pulsators that have a dominant period below 40 minutes [8]. Without information on the colour variations, it was not clear whether the observed variability was due to pulsations. For these reasons, we placed this object on the list of puzzling OGLE variables for a low-resolution spectroscopic follow-up in 2014. The spectrum obtained [9] was characterized by a continuum rising strongly to the blue, with superimposed hydrogen and helium lines indicating high effective temperature T_{eff} . It looked similar to those of moderately helium-enriched hot subdwarfs of O and B type (sdOB). By fitting a model atmosphere appropriate for typical hot subdwarfs, we found a temperature around 33,000 K, corresponding to spectral type O9, and surface gravity of $\log g \approx 5.3$ dex. This temperature is far too high for δ Sct-type stars, which have T_{eff} between 6,000 and 10,000 K or spectral types between A0 and F9. The high surface gravity ruled out the possibility that it could be a pulsating main-sequence star of β Cephei type. Moreover, pulsators of this type have periods at least three times as long and typically much lower amplitudes [10–12]. This is even more true for another hot main-sequence pulsators, slowly pulsating B (SPB) stars [13]. The high amplitude excluded the possibility that the star was an oscillating hot subdwarf. Typical amplitudes of the dominant modes in hot subdwarfs are of millimagnitudes or lower [14]. Our object varies much more rapidly and with much higher amplitude than two known radially pulsating extreme helium stars, BX Cir and V652 Her, which have periods of 2.6 h and V -band amplitudes of about 0.1 mag [15, 16]. These stars are low-mass supergiants of spectral type B with atmospheres exceptionally poor in hydrogen ($< 0.1\%$). The observed properties of OGLE-GD-DSCT-0058 do not fit any known type of variable star [17–19].

Our recent search for short-period variables conducted in OGLE fields in the Galactic Bulge has brought about the discovery of another 13 objects with almost identical photometric behaviour (Fig. 1). The periods of these variables range from about 22 to 39 min, and their I -band amplitudes are between 0.19 and 0.36 mag. Such high amplitudes at such short periods are not observed in any known variables. All the light curves are very similar in shape: they show a fast increase and a slow decline which is very characteristic for fundamental-mode pulsators. In none of the new variables is amplitude modulation observed. Photometric scatter in some light curves results from a high number of observations and the presence of

close neighbouring stars of constant brightness in the images. All the variables exhibit only one period; we do not see any signs of binarity. The pulsational nature of the new variables can now be demonstrated by evident colour changes over the cycle (Fig. 2). The measured $V - I$ colour index variations are of 0.04 to 0.17 mag. The drop in the colour index covers approximately a quarter of the cycle and correlates with the brightness increase. Lower colour index results from higher effective temperature. This is observed in radially pulsating stars in which brightness variations are a consequence of regular temperature and radius variations.

All 14 detected variables form a homogeneous class of objects because of their extremely blue colour. Their position in the colour-magnitude diagrams for stars observed in the same fields clearly indicate high effective temperatures of the variables (Fig. 3). They are all located far blueward of the main-sequence stars of the same brightness. Based on the photometric properties of the new objects, which pulsate with exceptionally high amplitudes not previously observed earlier in any type of hot stars, we propose to call the whole class of variables ‘blue large-amplitude pulsators’ (BLAPs). We arranged the detected variables according to increasing right ascension and named them OGLE-BLAP-NNN, where NNN is a three-digit consecutive number. We rename the variable discovered in 2013 as OGLE-BLAP-001, and henceforth we propose to treat it as the prototype object of the whole class introduced here.

In 2016, we obtained a pair of moderate-resolution spectra of OGLE-BLAP-001, exposed one after another, each covering about 53% of the period. The spectra were taken around anti-phases of the cycle to investigate parameter changes. Based on follow-up photometry for this object, also obtained in 2016, we were able to verify phase coverage of the new spectra (Fig. 4). The first spectrum covered most of the fading branch down to the minimum brightness, and the second one covered the whole rising branch and a short part of the fading branch. Our new spectra confirm that there are temperature variations driven by pulsations. Neutral helium lines clearly change their depth and shape; the ionized helium line He II 4,686 Å appears stronger in the second spectrum when the object was hotter. The effective temperature—derived from fitting model atmospheres—varied from 28,600 to 33,100 K: that is, by about 13%. Owing to rapid variations of the physical parameters of the star, the true amplitude of the temperature changes is likely to be higher. As observed in pulsating stars, higher temperature corresponds to the maximum brightness. The new higher-resolution spectra helped us to achieve a better estimate of the surface gravity in OGLE-BLAP-001. The obtained value of $\log g \approx 4.6$ dex is different from what is observed in upper-main-sequence stars ($\log g < 4.3$ dex [20]) and known sdOB stars (5.3–6.2 dex [21, 22]). The atmosphere of OGLE-BLAP-001 seems to be moderately rich in helium, with a helium-to-hydrogen number ratio of about 0.28.

In 2016, we also obtained low-resolution spectra of three other stars of the new class (Fig. 5): OGLE-BLAP-009, OGLE-BLAP-011 and OGLE-BLAP-014. Within the parameter uncertainties, the atmospheric properties of these stars are very similar to those of the prototype object. This shows that pulsations in BLAPs are excited under specific conditions.

The key to understanding the nature of the new pulsators is rates of period change rates determined from the long-term OGLE observations (Table 1). We estimate period changes for 11 objects. The rates are of the order of 10^{-7} yr^{-1} . Among six variables with significant period changes ($> 3\sigma$), the rates are negative in two stars, whereas they are positive in four objects. In three other stars, the changes are very likely positive

(with standard deviation between 2 and 3). Our observations show the long-term stability of the pulsation period in BLAPs.

The upper limit on absolute systematic rates of period change implies that we are dealing with objects slowly evolving on the nuclear timescale. As the main-sequence phase has been already excluded, one of the two remaining possibilities is the core helium-burning phase, the same as for classical Cepheids, RR Lyrae-type stars and sdOB stars. BLAPs pulsate in the fundamental mode like the first two types of pulsators, whereas their effective temperature is similar to the third type. The core helium-burning phase in hot stars may take place only if they suffer significant mass loss (about 75 %). This emphasises the connection to sdOB stars. However, although BLAPs and hot subdwarfs have comparable effective temperatures, as seen in Fig. 7, the two classes of hot stars differ significantly in luminosity, by an order of magnitude. Luminosity is inversely proportional to the surface gravity, and thus BLAPs have much lower gravity (by an order of magnitude) than hot subdwarfs. Relatively low gravity and high-amplitude pulsations point to the presence of inflated envelopes in the new pulsators.

To explore the idea of an inflated envelope, we have calculated a uniform envelope model adopting mean values of the parameters derived from our observations of the prototype object OGLE-BLAP-001 (Fig. 6). The observed helium-to-hydrogen ratio of $\log N(\text{He})/N(\text{H}) = -0.55$ dex translates to the hydrogen and helium mass fractions of $X = 0.46$ and $Y = 0.52$, respectively, assuming the solar metallicity of $Z = 0.02$. The model is calculated downward from the surface of the star to a temperature of $T = 2 \times 10^7$ K, low enough to neglect the hydrogen burning. Our model shows that a significant driving in the region of the metal opacity bump around $T \approx 2 \times 10^5$ K indeed occurs at the observed period of $P = 28.26$ min and surface temperature of $T_{\text{eff}} = 30,800$ K at star luminosity of about $\log L/L_{\odot} \approx 2.6$. According to stellar evolutionary models [23], such luminosity is generated within the helium-burning core of a mass of about $1.0 M_{\odot}$. It can be formed in the evolution of a star with the zero-age main sequence mass $M_{\text{ZAMS}} \approx 5 M_{\odot}$. Pulsations are confined to an extended acoustic cavity in the star envelope whose mass is only 2.5% of the total mass (Fig. 6). The excitation takes place in a narrow layer above the acoustic cavity around the Z-bump. This bump is not only responsible for driving pulsations in massive main-sequence B stars (β Cep and SPB type), but also in evolved stars such as sdOBs on the extreme horizontal branch. The cumulative work integral (W) at the bottom of the envelope is below zero, implying mode stability. This is expected because our model does not account for the radiative levitation of iron, which plays an important role in exciting pulsation modes in sdOB stars [24]. Importantly, the first overtone is even more stable, as W is lower than for the fundamental mode.

A lower mass loss is required for the second possibility: that is, BLAPs are stripped red giants with luminosities of about $\log L/L_{\odot} \approx 2.3$. In this case, the energy is produced in the hydrogen-burning shell above the degenerate helium core of a mass of $\sim 0.3 M_{\odot}$. Such a configuration takes place in stars of $M_{\text{ZAMS}} \approx 1 M_{\odot}$ before helium flash. The second model seems more likely not only because the requirements on mass loss are less severe, but also because it better reproduces the observed gravity (Table 2). Furthermore, we are closer to the fundamental mode instability. Gravities determined from the spectra for the three other pulsators are slightly lower than for the prototype object, but this is in agreement with their longer pulsation periods.

We may conclude that the pulsation properties of BLAPs are remarkably similar to those of classical

Cepheids and RR Lyrae-type stars. However, there is a connection to sdOBs, as our stars must have lost a significant fraction of the ZAMS mass to reach higher surface temperature and gravity, as measured. In the Hertzsprung-Russell diagram, the newly discovered pulsators occupy a space where no pulsating variables had previously been known (Fig. 7). In terms of driving properties, BLAPs are presumably related to the narrow instability domain recently found at somewhat lower temperatures [25]. More accurate measurements of the gravity would allow for an independent estimate of mass and luminosity, thus distinguishing between the two proposed models for the new pulsators. The derived luminosities of $\log L/L_{\odot} = 2.3$ and 2.6 for the prototype object OGLE-BLAP-001 translate to its absolute brightness M_V of +1.95 in the less massive case and +1.20 mag in the more massive case. Using the most recent extinction map [26], we find that all variables observed toward the Galactic bulge, except for the brightest object OGLE-BLAP-009, are located at distances between 6 and 12 kpc, that is, within the bulge. Assuming an intrinsic colour of the new pulsators of $(V - I)_0 = -0.29$ mag and the standard interstellar extinction law ($R_{V,VI} = 2.46$), we obtain the distance to the prototype variable of about 5.9 and 8.3 kpc, for the less massive case and the more massive one, respectively. OGLE-BLAP-009 is the closest of all pulsators. Like the prototype, it is located in the Galactic Disk. The calculated distance is either of about 2.9 or 4.1 kpc, for the less massive case and more massive one, respectively, assuming a higher luminosity of this object by 0.2 dex than in the prototype and non-standard extinction law ($R_{V,VI} = 2.14$) towards the Galactic Bulge [27].

The formation scenario of BLAPs remains a mystery. Rejection of a significant fraction of the stellar mass in the evolution of a single isolated low-mass star is impossible. Such a huge mass loss could take place during an encounter of the star with the central supermassive black hole. This has been proposed to solve the problem of the absence of luminous red giants in the inner parts of the Galactic Bulge [28]. Our variables, however, are not located close to the Galactic Centre. They seem to be distributed over the whole bulge and two of them reside in the Galactic Disk. Lines in the obtained spectra are almost unshifted with respect to their laboratory positions, indicating low radial velocities of BLAPs. This does not support a runaway scenario resulting from such an encounter. A more realistic explanation for the origin of our objects seems to be binary evolution through mass transfer and common envelope ejection. This is a widely accepted formation channel of sdB stars, as most of them are observed in binary systems [29]. It is supposed that single sdB stars are remnants of mergers between two helium white dwarfs [30]. In the case of BLAPs, we cannot exclude the possibility that some of them might be in binary systems with a companion faint enough to be detected in our data. The very small number of BLAPs in comparison, for instance, to several hundreds of known sdB stars, points to a rare episode in the stellar evolution.

Methods

Photometric observations and reductions

The OGLE project operates the 1.3-m Warsaw Telescope located at Las Campanas Observatory, Chile. Since the installation of a 32-detector mosaic CCD camera with 1.4 deg² field of view in 2010, the project has been in its fourth phase (OGLE-IV [1]). The previous phase (OGLE-III [31]) was conducted in the years 2001–2009. Observations are taken mainly in the *I* filter, whereas the *V* filter is used to secure colour information. The number of *I*-band measurements collected by OGLE-IV towards the Galactic Bulge in the years 2010–2016 varies greatly between individual fields, from about 100 observations in the least-sampled fields to over 14,000 observations in the most frequently monitored areas. Field cadence of the *I*-band data is from 20 min (or about 30 epochs per night) up to 2 days. The total number of collected *V*-band measurements is much smaller, between 8 and 140 observations. Reduction of the OGLE images is performed with the help of difference image analysis technique [32], which provides very accurate photometry in dense stellar fields (3% for 18 mag, 10% for 19.5 mag). The initial search for periodic variability in nearly 400 million *I*-band light curves from the Galactic Bulge was done using the publicly available FNPEAKS code for periods longer than 0.01 day. The blue large-amplitude pulsators presented here were serendipitously found during a visual inspection of light curves with a signal-to-noise ratio higher than 5 and periods below 0.22 days [33]. The TATRY code [34] was used for precise determination of the periods after converting the moments of observations from heliocentric Julian date (HJD) to the more accurate barycentric Julian date (BJD_{TDB}). We calculated the rate of the period change for objects observed both in OGLE-III and OGLE-IV as

$$r = \frac{\Delta P}{\Delta t} \frac{1}{P_{\text{IV}}} = \frac{P_{\text{IV}} - P_{\text{III}}}{t_{\text{IV}} - t_{\text{III}}} \frac{1}{P_{\text{IV}}}.$$

This simple method was used because of very small period changes observed in our new pulsators. We found that dividing the data into separate seasons did not lead to conclusive results.

An independent photometric campaign for the prototype object OGLE-BLAP-001, located in the Galactic Disk, was conducted in 2016. The campaign helped us to estimate the period change in this object after 10 years. It also allowed us to determine the phase coverage of our follow-up spectroscopic observations. The photometric data were obtained with the Direct CCD Camera on the 1.0-m Swope telescope at Las Campanas Observatory on the following four nights in 2016: 30–31 January, 2 February, and 26 April. A total of 229 *I*-band images with an exposure time of 120 s and 62 *V*-band images with exposure time 180 s were collected. All images were de-biased and flat-fielded using the IRAF package. The photometry was extracted with the help of difference image analysis. A reference frame was constructed by combining 11 individual images with seeing $\leq 1.5''$. Profile photometry for the reference frame was extracted with the DAOPHOT/ALLSTAR package [35]. We used these measurements to transform the light curve from differential flux units into magnitudes.

Spectroscopic observations and reductions

The pair of spectra of the prototype object OGLE-BLAP-001 was obtained with the 6.5-m Magellan-Baade telescope at the Las Campanas Observatory on 22 April 2016. We used the Magellan Echellette (MagE)

spectrograph with a slit $10''$ long and $1.0''$ wide, giving an average spectral resolution of $R \approx 4100$ and covering wavelengths between 3,200 and 10,000 Å. Each spectrum was exposed for 900 s with a read-out time of 30 s. Based on photometry from the Swope telescope, we conclude that the spectra were taken in the following phase ranges: 0.162–0.693 and 0.711–1.242. Initial reductions (that is, flat-field correction, rectification of spectral orders and wavelength calibration) were done with the CarPy software on the site. In the next step, the orders were normalized and combined using utilities provided in the IRAF package.

The low-resolution spectroscopic follow-up of objects OGLE-BLAP-009, OGLE-BLAP-011, and OGLE-BLAP-014 was performed at the 8.1-m Gemini-South telescope with the Gemini Multi-Object Spectrograph (GMOS) under programme GS-2016A-Q-71 (Principal Investigator R. Angeloni). The observations were conducted in regular queue mode between March and June 2016 on gray nights (V -band sky brightness > 19.5 mag arcsec $^{-2}$), no photometric conditions (maximum extinction of 0.3 mag over the nominal atmospheric one) and seeing $\lesssim 1.1''$. GMOS was configured with the $1.0''$ slit and the B600_G5323 grating centered at 5,500 Å, capable of delivering a resolution of $R \approx 800$ over a wavelength range of 4,000–7,000 Å. Four 300 s exposures were taken for each target following an optimized spatial and spectral dithering pattern: it aimed at filling the small gaps in both the spatial and spectral coverage due to the slit bridges (necessary in order to keep the $330''$ -long slit stable) and due to the gaps between the detectors, respectively. The data frames were finally processed with the Gemini IRAF package (v1.13.1 under Ureka v1.5.1) following the standard procedures for long-slit data reduction.

The spectra were fitted with line-blanketed non-local thermodynamic equilibrium (non-LTE) model atmospheres computed using the public codes TLUSTY and SYNSPEC assuming a plane-parallel geometry [36]. The model grid covers the following parameter ranges: $20,000 \text{ K} < T_{\text{eff}} < 50,000 \text{ K}$, $4.6 < \log g < 6.4$, and $-4.0 < \log N(\text{He})/N(\text{H}) < 0.0$. The metallic elements included in the models follow a typical abundance for hot subdwarfs [37]: solar abundances for N, S and Fe, and one tenth solar for C, O and Si. The best-fit parameters are obtained via a χ^2 minimization procedure that relies on the method of Levenberg-Marquardt, based on a steepest-descent method [38]. Normalised hydrogen as well as helium lines of both the observed and model spectra (previously convolved with a Gaussian matching the observed resolution) are thus compared.

The same procedure was used for fitting the Gemini-South spectra of the three follow-up objects; however, for these stars our initial fits indicated surface gravities outside the lower limit of our grid ($\log g < 4.6$). To avoid extrapolation, we recomputed an extended grid, this time covering the range $3.8 < \log g < 5.6$. These new models are computed in non-LTE but only include opacity from hydrogen and helium, because computing a grid of fully line-blanketed models requires a considerable time. We expect the effect of metallicity on the derived parameters to be rather small for effective temperatures below 35,000 K [39], and, given the modest signal-to-noise ratio of the spectra, the formal fitting uncertainties are much larger than any systematic that could be caused by the metallicity of the models.

Model of the envelope

To investigate radial-mode stability in the new pulsators, we applied a linear non-adiabatic equilibrium envelope model [40] updated for the use of modern atomic data (OPAL opacities [41]). A standard ratio of mixing length to pressure scale-height $\alpha = 1.5$ was adopted. The effect of rotation was ignored. The envelope model was calculated for various star masses assuming radial F-mode pulsations with $P_F = 0.01962$ d,

effective temperature of 30,800 K ($\log T_{\text{eff}} = 4.48855$) and uniform chemical composition with abundances derived for the prototype object OGLE-BLAP-001. Pulsations are regarded as a small departure from the dynamical and thermal equilibrium [42]. The period is insensitive to the interior as long as the Brunt-Väisälä frequency at the envelope base, N , exceeds the mode frequency, $\omega_F = 2\pi/P_F$.

References

- [1] Udalski, A., Szymański, M. K. & Szymański, G. OGLE-IV: fourth phase of the Optical Gravitational Lensing Experiment. *Acta Astron.* **65**, 1-38 (2015).
- [2] Soszyński, I. *et al.* The Optical Gravitational Lensing Experiment. The OGLE-III Catalog of Variable Stars. XV. Long-Period Variables in the Galactic Bulge. *Acta Astron.* **63**, 21-36 (2013).
- [3] Soszyński, I. *et al.* Over 38000 RR Lyrae Stars in the OGLE Galactic Bulge Fields. *Acta Astron.* **64**, 177-196 (2014).
- [4] Soszyński, I. *et al.* The OGLE Collection of Variable Stars. Classical Cepheids in the Magellanic System. *Acta Astron.* **65**, 297-312 (2015).
- [5] Soszyński, I. *et al.* The OGLE Collection of Variable Stars. Over 450 000 Eclipsing and Ellipsoidal Binary Systems Toward the Galactic Bulge. *Acta Astron.* **66**, 405-420 (2016).
- [6] Mróz, P. *et al.* One Thousand New Dwarf Novae from the OGLE Survey. *Acta Astron.* **65**, 313-328 (2015).
- [7] Pietrukowicz, P. *et al.* Large Variety of New Pulsating Stars in the OGLE-III Galactic Disk Fields. *Acta Astron.* **63**, 379-404 (2013).
- [8] Rodríguez, E., López-González, M. J. & López de Coca, P. A revised catalogue of delta Sct stars. *Astron. Astrophys. Suppl.* **144**, 469 (2000).
- [9] Pietrukowicz, P. *et al.* A Low-Resolution Spectroscopic Exploration of Puzzling OGLE Variable Stars. *Acta Astron.* **63**, 63-79 (2015).
- [10] Stankov, A. & Handler, G. Catalog of Galactic β Cephei Stars. *Astrophys. J. Suppl. Ser.* **158**, 193-216 (2005).
- [11] Pigulski, A. & Pojmański, G. β Cephei stars in the ASAS-3 data. I. Long-term variations of periods and amplitudes. *Astron. Astrophys.* **477**, 907-915 (2008).
- [12] Pigulski, A. & Pojmański, G. β Cephei stars in the ASAS-3 data. II. 103 new β Cephei stars and a discussion of low-frequency modes. *Astron. Astrophys.* **477**, 917-929 (2008).
- [13] De Cat, P. Observational Asteroseismology of slowly pulsating B stars. *Comm. in Asteroseismology* **150**, 167-174 (2007).
- [14] Heber, U. Hot Subluminous Stars. *Pub. of Astron. Soc. of Pacific* **128**, 082001 (2016).

- [15] Woolf, V. M. & Jeffery, C. S. Temperature and gravity of the pulsating extreme helium star LSS 3184 (BX Cir) through its pulsation cycle. *Astron. Astrophys.* **395**, 535-540 (2002).
- [16] Jeffery, C. S. *et al.* Subaru and Swift observations of V652 Herculis: resolving the photospheric pulsation. *Mon. Not. R. Astron. Soc.* **447**, 2836-2851 (2015).
- [17] Christensen-Dalsgaard, J. An Overview of Helio- and Asteroseismology in Proc. of the SOHO 14 / GONG 2004 Workshop (ESA SP-559): Helio- and Asteroseismology: Towards a Golden Future (ed. Danesy, D.) 1-33 (New Haven, Connecticut, USA, 2004).
- [18] Eyer, L. & Mowlavi, N. Variable stars across the observational HR diagram in Journal of Physics: Conf. Ser., **118**, 012010 (2008).
- [19] Catelan, M. & Smith, H. A. *Pulsating Stars* (Wiley-VCH, 2015).
- [20] Pamyatnykh, A. A. Pulsational Instability Domains in the Upper Main Sequence. *Acta Astron.* **49**, 119-148 (1999).
- [21] Edelmann, H. *et al.* Spectral analysis of sdB stars from the Hamburg Quasar Survey. *Astron. Astrophys.* **400**, 939 (2003).
- [22] Randall, S. K. *et al.* Pulsating hot O subdwarfs in ω Centauri: mapping a unique instability strip on the extreme horizontal branch. *Astron. Astrophys.* **589**, A1 (2016).
- [23] Pietrinferni, A., Cassisi, S., Salaris, M., & Castelli, F. A Large Stellar Evolution Database for Population Synthesis Studies. II. Stellar Models and Isochrones for an α -enhanced Metal Distribution. *Astron. Astrophys.* **642**, 797-812 (2006).
- [24] Charpinet, S. *et al.* A Driving Mechanism for the Newly Discovered Class of Pulsating Subdwarf B Stars. *Astrophys. J.* **483**, L123-L126 (1997).
- [25] Jeffery, C. S. & Saio, H. Radial pulsation as a function of hydrogen abundance. *Mon. Not. R. Astron. Soc.* **458**, 1352-1373 (2016).
- [26] Nataf, D. M. *et al.* Reddening and Extinction toward the Galactic Bulge from OGLE-III: The Inner Milky Way's $R_V \sim 2.5$ Extinction Curve. *Astrophys. J.*, **769**, 88 (2013)
- [27] Udalski, A. The Optical Gravitational Lensing Experiment: Is Interstellar Extinction toward the Galactic Center Anomalous? *Astrophys. J.*, **590**, 284-290 (2003)
- [28] Kieffer, T. F. & Bogdanović, T. Can Star-Disk Collisions Explain the Missing Red Giants Problem in the Galactic Center? *Astrophys. J.*, **823**, 155 (2016)
- [29] Han, Z., Podsiadlowski, P., Maxted, P. F. L., Marsh, T. R. & Ivanova, N. The origin of subdwarf B stars – I. The formation channels. *Mon. Not. R. Astron. Soc.*, **336**, 449 (2002)
- [30] Hall, P. D. & Jeffery, C. S. Hydrogen in hot subdwarfs formed by double helium white dwarf mergers. *Mon. Not. R. Astron. Soc.*, **463**, 2756 (2016)

- [31] Udalski, A., Szymański, M. K., Soszyński, I., & Poleski, R. The Optical Gravitational Lensing Experiment. Final Reductions of the OGLE-III Data. *Acta Astron.* **58**, 69-87 (2008).
- [32] Woźniak, P. R. Difference Image Analysis of the OGLE-II Bulge Data. I. The Method *Acta Astron.* **50**, 421-450 (2000).
- [33] Soszyński, I. *et al.* Ultra-Short-Period Binary Systems in the OGLE Fields Toward the Galactic Bulge. *Acta Astron.* **65**, 39-62 (2015).
- [34] Schwarzenberg-Czerny, A. Fast and Statistically Optimal Period Search in Uneven Sampled Observations. *Astrophys. J.* **460**, L107-L110 (1996).
- [35] Stetson, P. B. DAOPHOT—A computer program for crowded-field stellar photometry. *Publ. Astron. Soc. Pacif.* **99**, 191-222 (1987).
- [36] Lanz, T. & Hubeny, I. Non-LTE line-blanketed model atmospheres of hot stars. 2: Hot, metal-rich white dwarfs. *Astrophys. J.* **439**, 905-916 (1995).
- [37] Blanchette, J.-P. *et al.* FUSE Determination of Abundances in Long-Period Pulsating V1093 Her (PG 1716+426) Stars. *Astrophys. J.* **678**, 1329-1341 (2008).
- [38] Saffer, R. A., Bergeron, P., Koester, D., & Liebert, J. Atmospheric parameters of field subdwarf B stars. *Astrophys. J.* **432**, 351-366 (1993).
- [39] Latour, M., Fontaine, G., Green, E. M., Brassard, P., & Chayer, P. Improved Determination of the Atmospheric Parameters of the Pulsating sdB Star Feige 48. *Astrophys. J.* **788**, 65 (2014).
- [40] Paczyński, B. Envelopes of Red Supergiants. *Acta Astron.* **19**, 1-22 (1969).
- [41] Iglesias, C. A. & Rogers, F. J. Updated Opal Opacities. *Astron. Astrophys.* **464**, 943-953 (1996).
- [42] Dziembowski, W. Oscillations of giants and supergiants. *Acta Astron.* **27**, 95-126 (1977).

Correspondence Correspondence and requests for materials should be addressed to P.P. (pietruk@astrouw.edu.pl).

Acknowledgements We thank M. Kubiak and G. Pietrzyński, former members of the OGLE team, for their contribution to the collection of the OGLE photometric data over the past years. The OGLE project has received funding from the National Science Centre, Poland (grant number MAESTRO 2014/14/A/ST9/00121 to A.U.). M.L. acknowledges support from the Alexander von Humboldt Foundation. The Las Campanas Observatory, which hosts the Warsaw Telescope, Swope Telescope and Magellan Telescopes is operated by the Carnegie Institution for Science. The Gemini Observatory is operated by the Association of Universities for Research in Astronomy, Inc., under a cooperative agreement with the NSF on behalf of the Gemini partnership: the National Science Foundation (United States), the National Research Council (Canada), CONICYT (Chile), Ministerio de Ciencia, Tecnología e Innovación Productiva (Argentina), and Ministério da Ciência, Tecnologia, Inovações e Comunicações (Brazil).

Author contributions P.P. coordinated the research, obtained and analysed part of the observations and prepared the manuscript. W.A.D. proposed the envelope model and calculated its characteristics. M.L. fitted model atmospheres to the spectroscopic data. R.A. obtained and reduced Gemini spectra. R.P. and F.diM. obtained part of the follow-up photometric observations. The remaining authors, including also P.P. and R.P., collected the OGLE observations. All authors commented on the manuscript and were involved in the science discussion.

Data Availability Statement The data that support the plots within this paper and other findings of this study are available from the corresponding author upon reasonable request. The time-series photometry of the new variables is available to the astronomical community from the OGLE Internet Archive at <ftp://ftp.astrouw.edu.pl/ogle/ogle4/OCVS/BLAP/>

Competing interests The authors declare no competing financial interests.

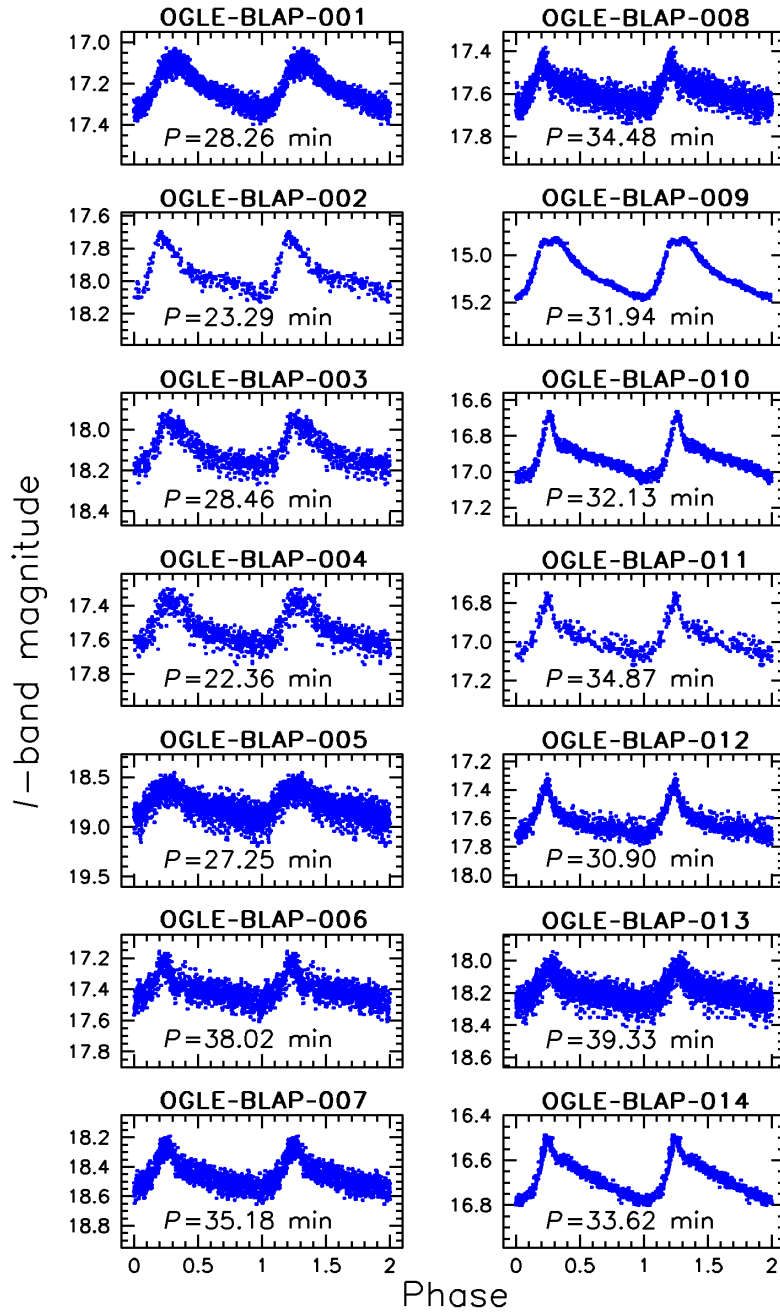


Figure 1: **Phased I -band light curves of blue large-amplitude pulsators (BLAPs) detected by the OGLE survey.** Period, P , is given for each object. The light curve shapes of the new variables are remarkably similar to the shapes of δ Sct, RR Lyrae and δ Cep-type stars pulsating in the fundamental mode, but those have much longer periods.

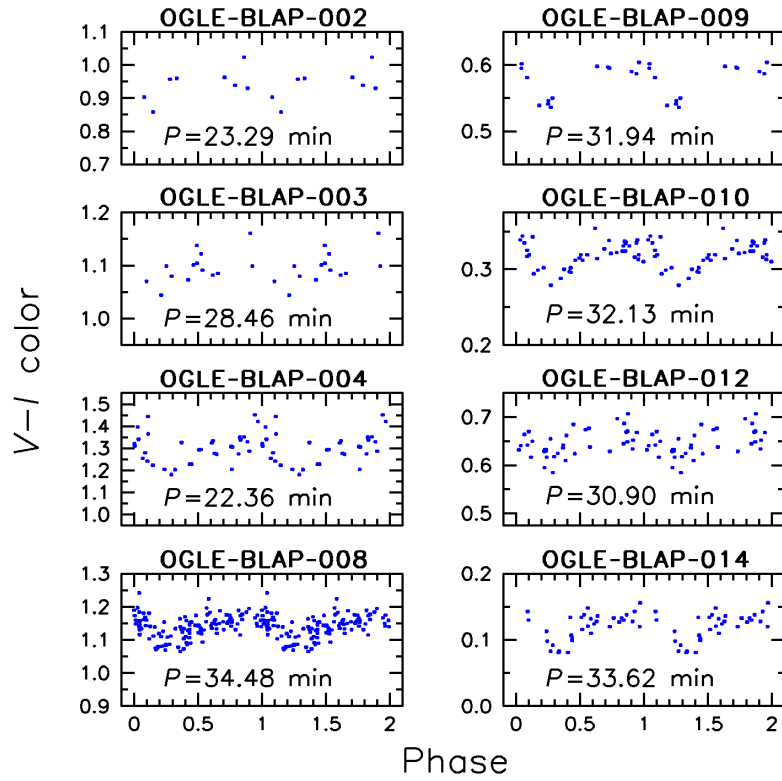


Figure 2: **Variations of the $V - I$ colour over the cycle in the new variable stars.** This certifies that the observed variability is driven by physical changes in the star, that is, by pulsations.

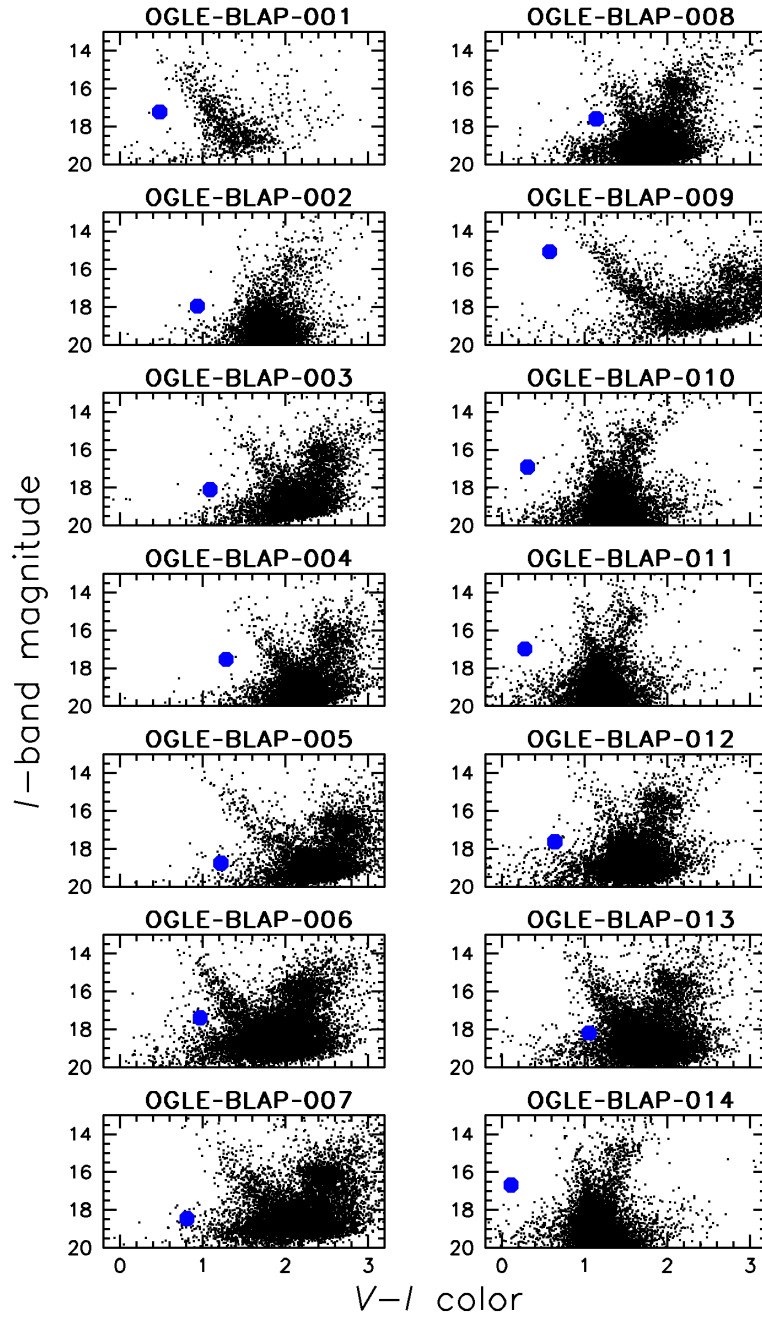


Figure 3: **Colour-magnitude diagrams for stars in the fields with detected BLAPs.** Large circles mark mean positions of the variables. Observed brightness and colour variations are roughly of the size of the blue circles. The new pulsators have significantly bluer colour than main-sequence stars of the same brightness, which form the left branch of the V-shaped structure.

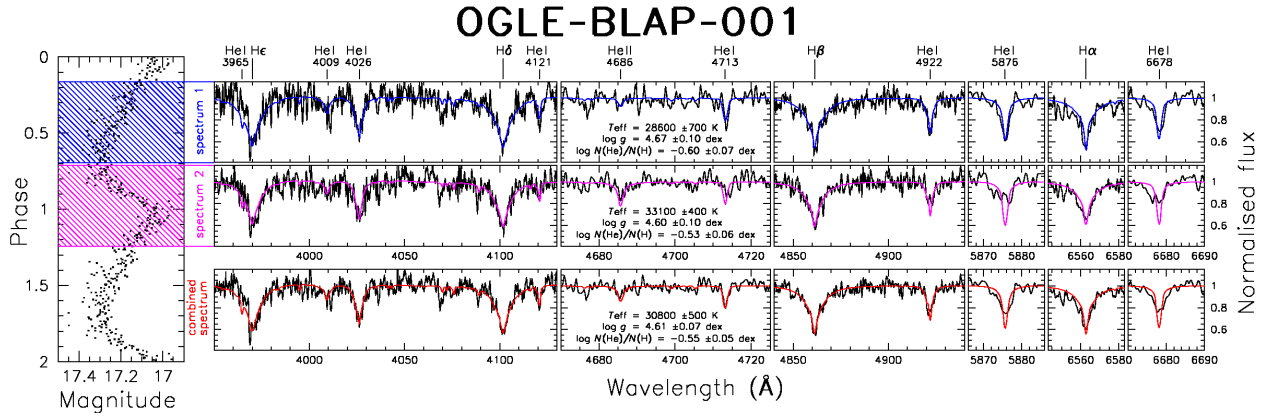


Figure 4: **Magellan-Baade moderate-resolution spectra at opposite phases of the cycle of the prototype object OGLE-BLAP-001.** Best fits of stellar atmosphere models to the observed spectra are shown by colour lines. The different effective temperatures derived indicate that the observed variability is indeed caused by pulsations. With increasing temperature, lines of ionized elements become stronger, for example He II 4,686 Å. Short-period pulsations result in striking changes in the shape of neutral helium lines (He I). Parameters derived from the combined spectrum can be treated as mean values for this prototype object. The uncertainties shown are formal errors returned by the χ^2 fitting procedure.

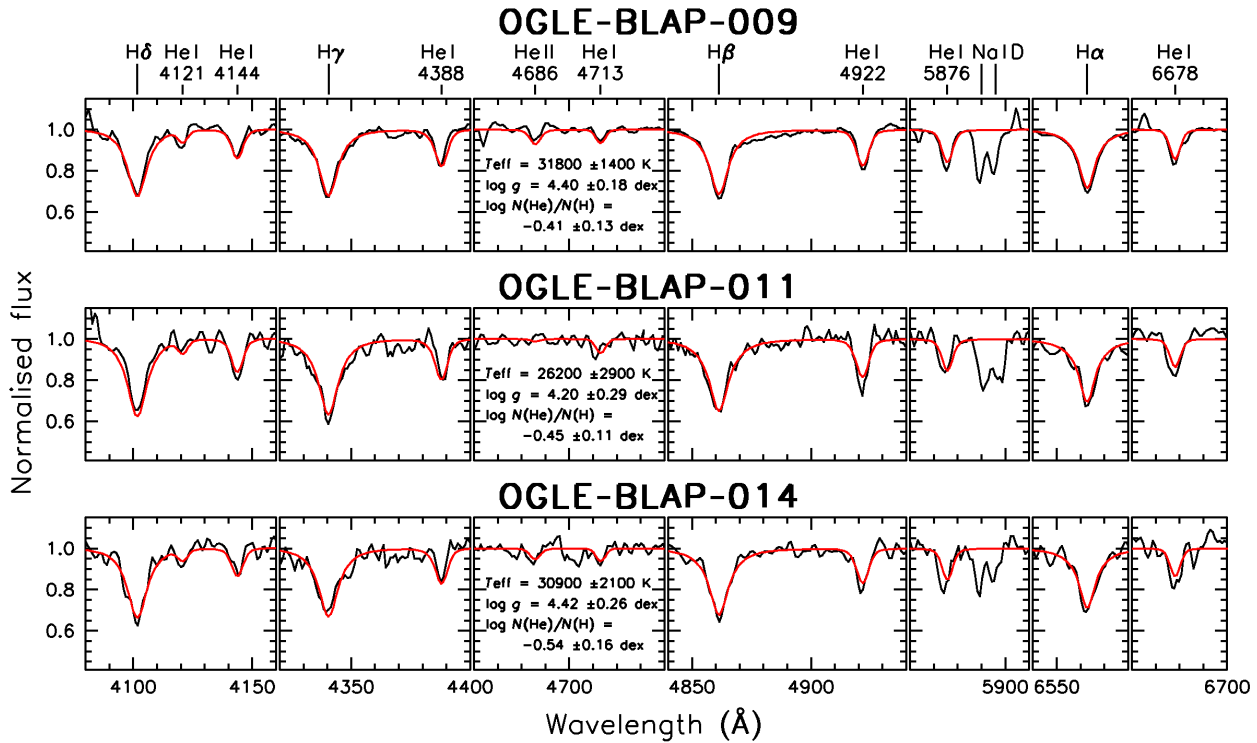


Figure 5: **Gemini-South low-resolution spectra for three BLAPs.** In the segments, small ticks are every 10 \AA . Best fits of stellar atmosphere models are shown with red lines. The sodium doublet (Na I D) is of interstellar origin. The uncertainties are formal errors returned by the χ^2 fitting procedure. Effective temperatures, surface gravities, and helium abundances derived for these stars are similar to the values obtained from moderate-resolution spectra for the prototype object OGLE-BLAP-001. This shows that all the newly discovered variables form a homogeneous class of objects.

Table 1: Observational parameters of the discovered BLAPs: equatorial coordinates, mean brightness and amplitude in the V and I bands, pulsation period, and rate of the period change. The rate and its uncertainty is calculated based on two epochs representing the third and the fourth (current) phase of the OGLE survey from years 2001–2009 and 2010–2016, respectively.

Variable name	RA(2000.0) (^h : ^m : ^s)	Dec(2000.0) ([°] : ['] : ^{''})	$\langle V \rangle$ (mag)	$\langle I \rangle$ (mag)	A_V (mag)	A_I (mag)	P (min)	r ($\times 10^{-7} \text{ y}^{-1}$)
OGLE-BLAP-001	10:41:48.77	−61:25:08.5	17.706	17.223	0.411	0.236	28.26	+2.9 ± 3.7
OGLE-BLAP-002	17:43:58.02	−19:16:54.1	18.892	17.953	0.317	0.357	23.29	
OGLE-BLAP-003	17:44:51.48	−24:10:04.0	19.195	18.103	0.273	0.229	28.46	+0.82 ± 0.32
OGLE-BLAP-004	17:51:04.72	−22:09:03.4	18.813	17.528	0.426	0.261	22.36	
OGLE-BLAP-005	17:52:18.73	−31:56:35.0	19.989	18.767	0.333	0.298	27.25	+0.63 ± 0.26
OGLE-BLAP-006	17:55:02.88	−29:50:37.5	18.354	17.384	0.279	0.231	38.02	−2.85 ± 0.31
OGLE-BLAP-007	17:55:57.52	−28:52:11.0	19.268	18.456	0.330	0.282	35.18	−2.40 ± 0.51
OGLE-BLAP-008	17:56:48.26	−32:21:35.6	18.732	17.590	0.284	0.194	34.48	+2.11 ± 0.27
OGLE-BLAP-009	17:58:48.20	−27:16:53.7	15.650	15.071	0.286	0.241	31.94	+1.63 ± 0.08
OGLE-BLAP-010	17:58:59.22	−35:18:07.0	17.231	16.919	0.383	0.344	32.13	+0.44 ± 0.21
OGLE-BLAP-011	18:00:23.24	−35:58:03.1	17.254	16.977	0.222	0.286	34.87	
OGLE-BLAP-012	18:05:44.20	−30:11:15.2	18.263	17.622	0.350	0.343	30.90	+0.03 ± 0.15
OGLE-BLAP-013	18:05:52.70	−26:48:18.0	19.244	18.190	0.249	0.221	39.33	+7.65 ± 0.67
OGLE-BLAP-014	18:12:41.79	−31:12:07.8	16.793	16.680	0.339	0.264	33.62	+4.82 ± 0.39

Table 2: Derived parameters of the envelope model for various star masses. The bottom of the envelope is placed at the radius $r = r_{\text{core}}$ where temperature is 2×10^7 K. Normalized driving rate η is calculated for the fundamental mode (F) and first overtone (1O). The two versions of evolutionary models consistent with similar values of $L(M_{\text{core}})$ are given in the last column. Heavy $\sim 1.0 M_{\odot}$ helium cores are formed in the evolution of stars with $M_{\text{ZAMS}} \approx 5 M_{\odot}$. In this case, a huge mass loss is required to create a BLAP. A much lower mass loss is needed if the BLAPs are shell hydrogen-burning objects with degenerate helium cores. At $M = 0.3 M_{\odot}$, the core has similar mass and luminosity as a $M_{\text{ZAMS}} \approx 1 M_{\odot}$ star on the red giant branch well before helium flash.

M/M_{\odot}	$\log T_{\text{eff}}$	$\log L/L_{\odot}$	$\log g$	$M_{\text{core}}/M_{\odot}$	r_{core}/R	η_{F}	$\eta_{1\text{O}}$	Model
0.30	4.4886	2.2572	4.5496	0.2983	0.1061	-0.239	-0.473	shell H-burning
0.35	4.4886	2.3039	4.5710	0.3474	0.1161	-0.230	-0.417	
0.40	4.4886	2.3440	4.5901	0.3963	0.1255	-0.225	-0.380	
0.45	4.4886	2.3787	4.6073	0.4450	0.1343	-0.223	-0.354	
0.50	4.4886	2.4097	4.6229	0.4934	0.1427	-0.222	-0.334	
0.60	4.4886	2.4626	4.6500	0.5893	0.1582	-0.224	-0.306	core He-burning
0.80	4.4886	2.5466	4.6926	0.7777	0.1852	-0.234	-0.275	
1.00	4.4886	2.6123	4.7250	0.9613	0.2083	-0.247	-0.261	
1.20	4.4886	2.6659	4.7509	1.1399	0.2286	-0.258	-0.254	

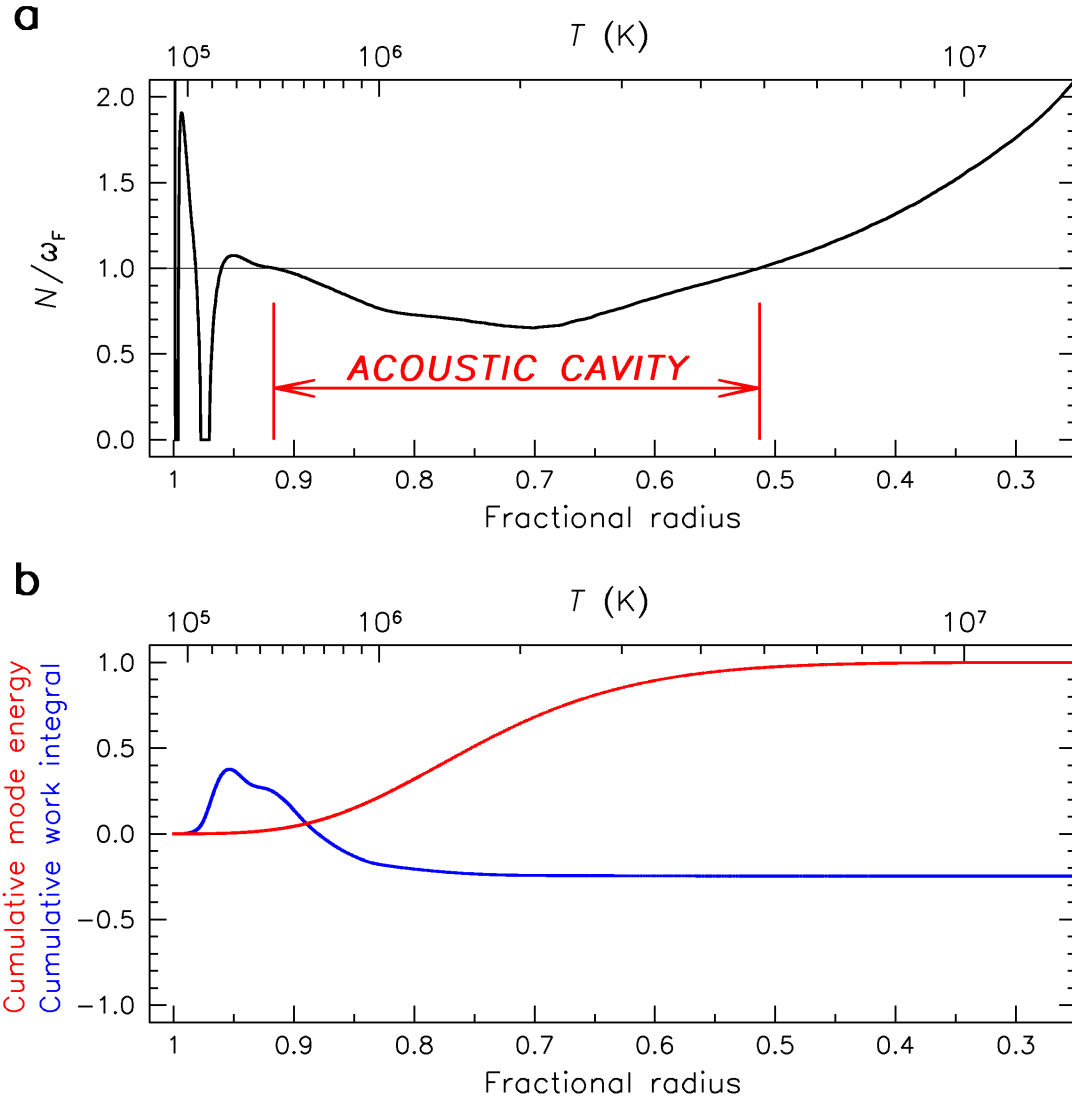


Figure 6: **Proposed envelope model for the new pulsators.** **a**, Pulsations are confined to an extended acoustic cavity in the star envelope where the ratio of Brunt-Väisälä frequency to the fundamental-mode frequency $N/\omega_F < 1$. The bottom of the envelope is located very deep, at about 0.25 of the star radius from its center or at a temperature of $T \approx 2 \times 10^7$ K. Hence, the star possesses a giant-like structure. In this sense, it is similar to Cepheids and RR Lyrae-type stars in which low-order radial modes are preferred. **b**, Nearly total contribution to the mode energy (red line) comes from the acoustic cavity. The driving effect arises in a narrow evanescent layer above the acoustic cavity around the maximum of the iron opacity at $T \approx 2 \times 10^5$ K. The damping takes place close to the surface of the star where the work declines (blue line). At the bottom of the envelope, the work drops below zero, implying mode stability. Our simplistic model ignores the iron levitation.

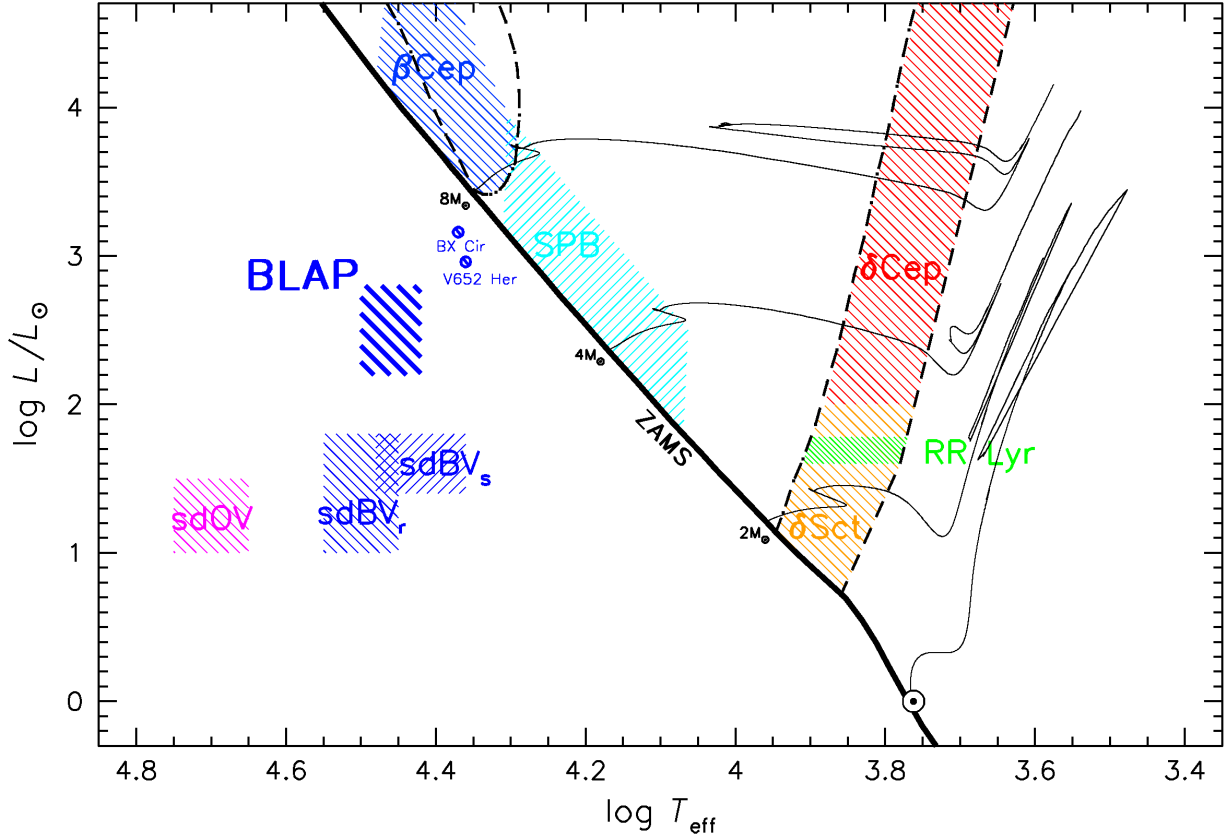


Figure 7: **Location of the BLAPs in the Hertzsprung-Russell diagram.** The zero-age main sequence (thick solid line), evolutionary tracks for 1, 2, 4 and 8 M_{\odot} (thin solid lines, [23]), edges of the classical instability strip and instability domain for radial pulsations in the upper main sequence (dashed lines, [20]) are presented for the metallicity of $Z = 0.02$. Hatched regions show locations of various types of known pulsating stars in which pulsations are driven by the presence of He II bump (δ Cep, δ Sct, and RR Lyrae-type stars) and Z bump in the opacity (β Cep-type, SPB stars, sdO, slowly (s) and rapidly (r) pulsating sdB variables). Different shading represents different types of modes: backslash (\) shading is for pressure modes whereas slash (/) shading is for gravity modes. Positions of two known radially pulsating extreme helium stars (BX Cir and V652 Her) are also marked (small circles). BLAPs are located in a region not occupied by any known pulsating variables.